A coupled flow - geomechanics study on the effectiveness of methane drainage in multi-seam coal mine with the use of long-reach directional drilling

Małgorzata Słota-Valim
Wiesław Szott
Piotr Łętkowski
Piotr Ruciński
Krzysztof Miłek

DD-MET

POLSKA GRUPA GÓRNICZA
Imperial College London
GIG
Universidad de Oviedo
Universidá d'Uviéu
University of Oviedo

2022 International Pittsburgh Coal Conference

STUDY LOCATION AND OBJECTIVES

OBJECTIVES

aims to assess the effectiveness of the coal mine methane drainage in the multi–seam coal mine situated within the Upper Silesian Coal Basin (USCB) in Poland using the long reach horizontal boreholes and cross measure boreholes.

Determination of the effectiveness of the CMM drainage is carried out using numerical methods coupling geomechanics with the modeling of the reservoir fluid flow.

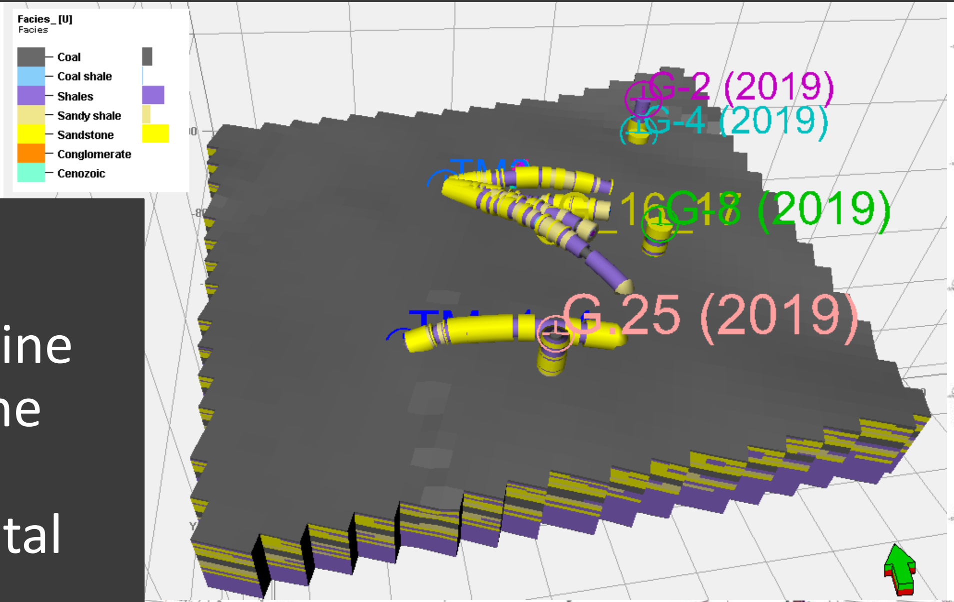

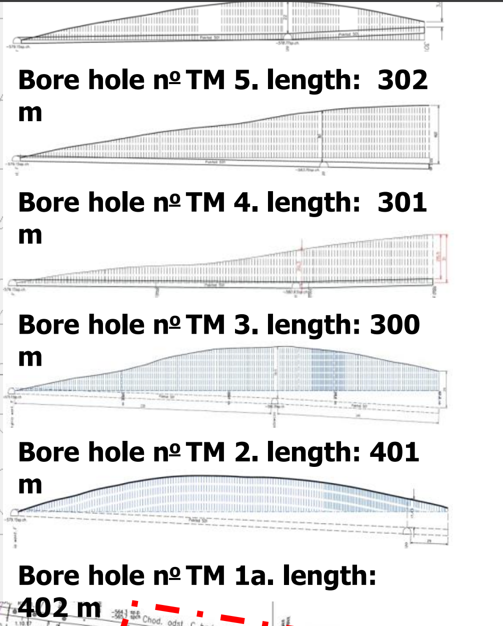

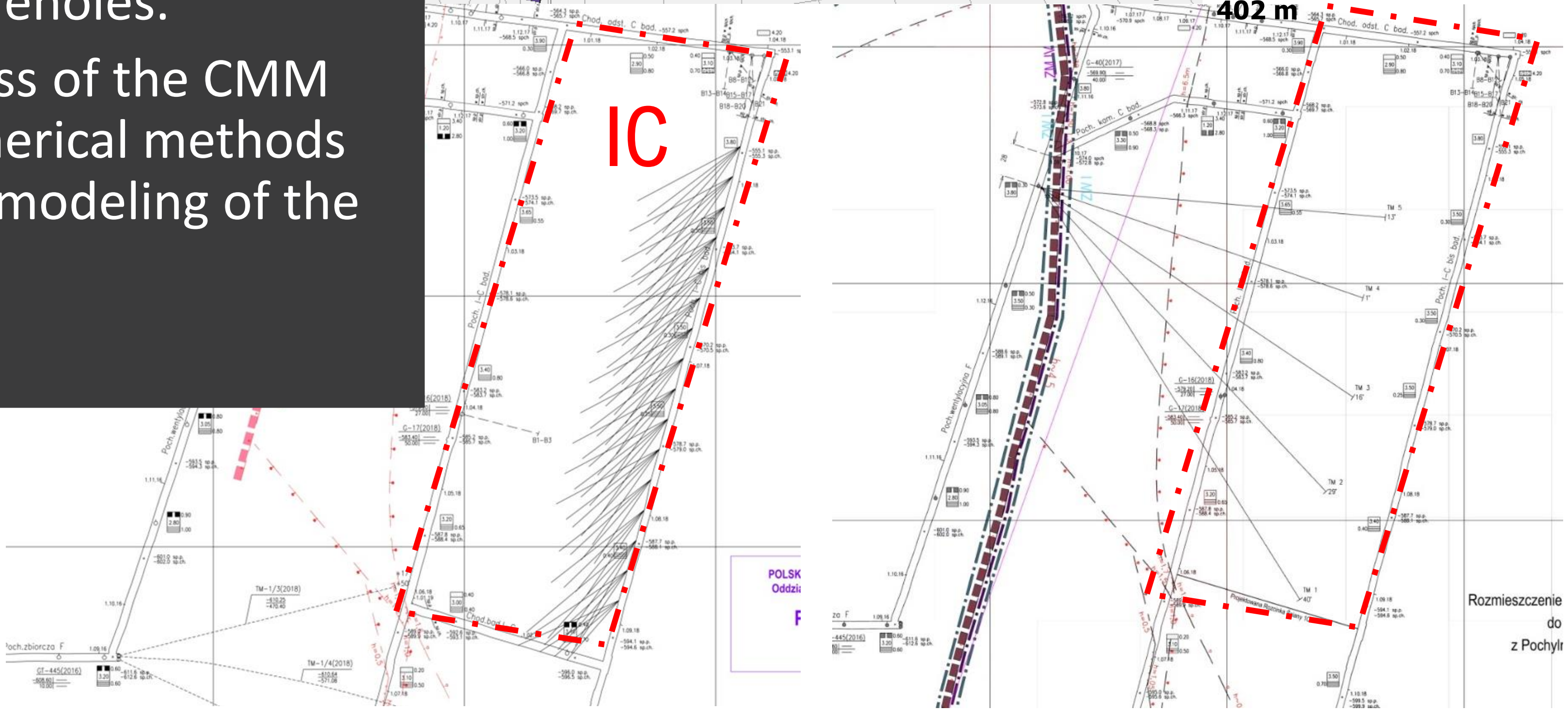

STUDY LOCATION AND OBJECTIVES

Fig. 1. Location of the study area in the vicinity of the I-C longwall marked with the red polygon with five horizontal degassing b orehole system visualized on the structural map of the coal seam (CS) 501 bottom within the C field in the Staszic-Wujek Coal Mine limited with major faults (A) and the interval of the interest subjected to the drainage (B).

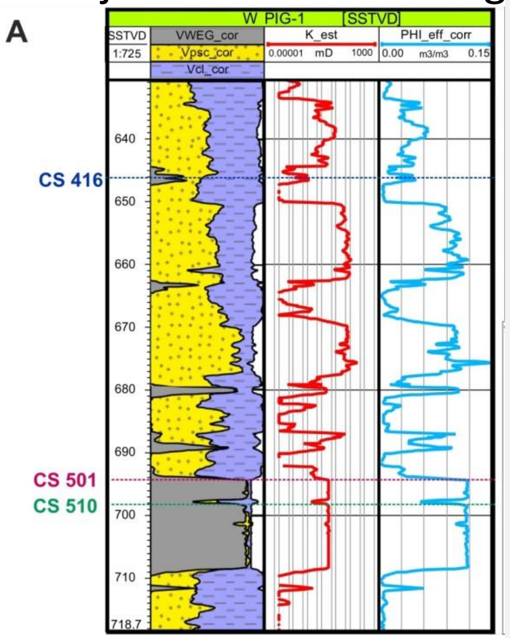

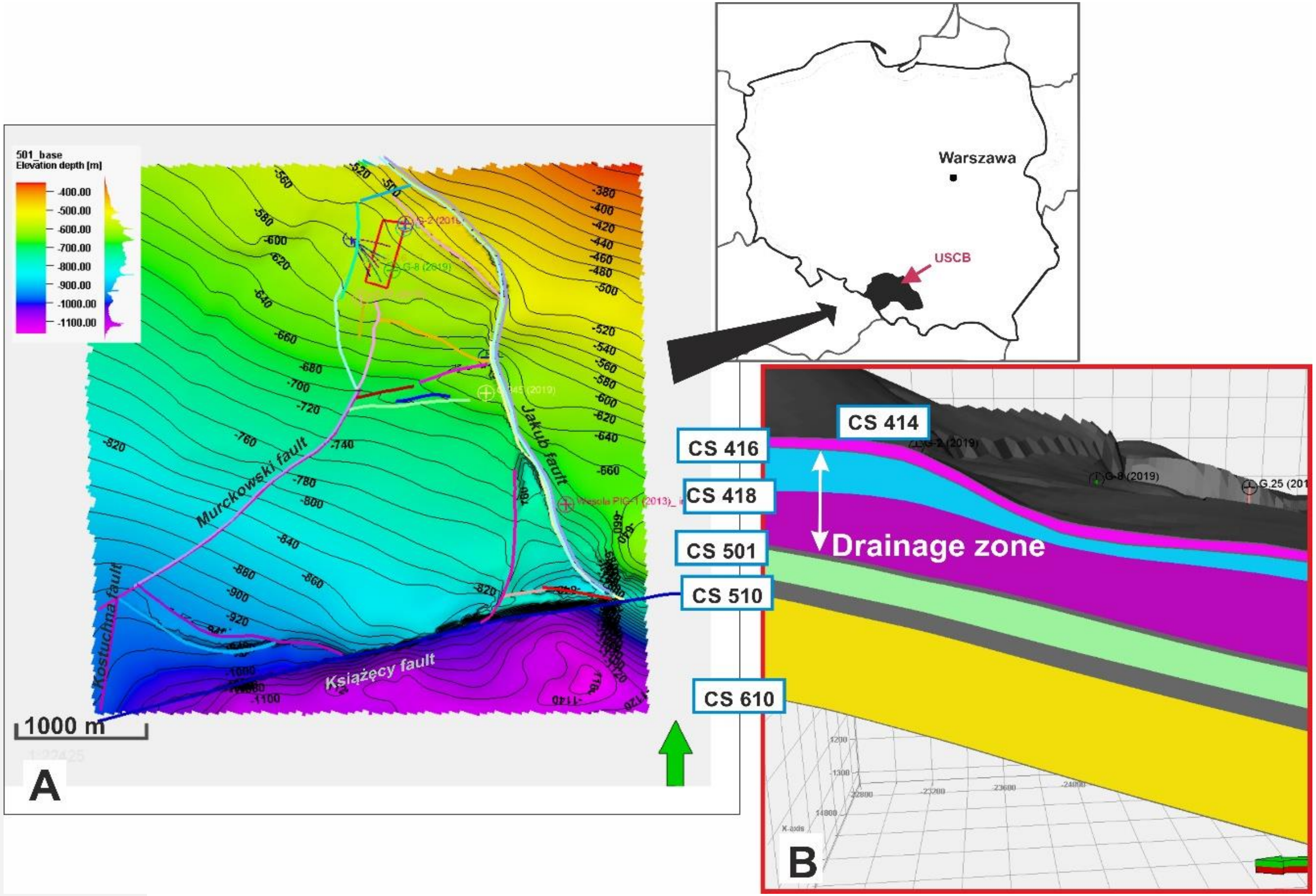

METHODOLOGY

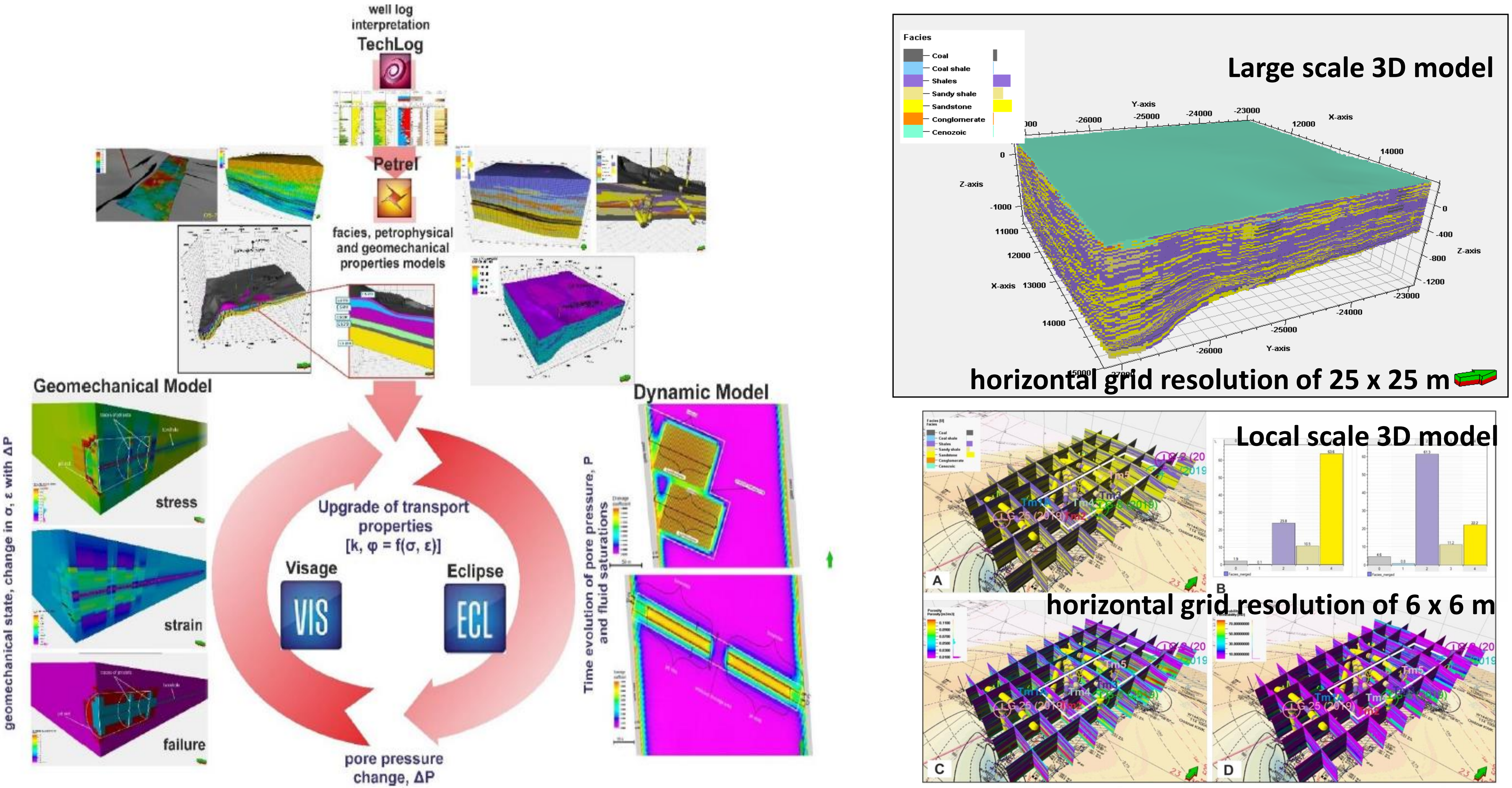

Figure. 2. Integrated geological geomechanical and fluid flow modelling and simulation workflow

3D STRUCTURAL MODEL

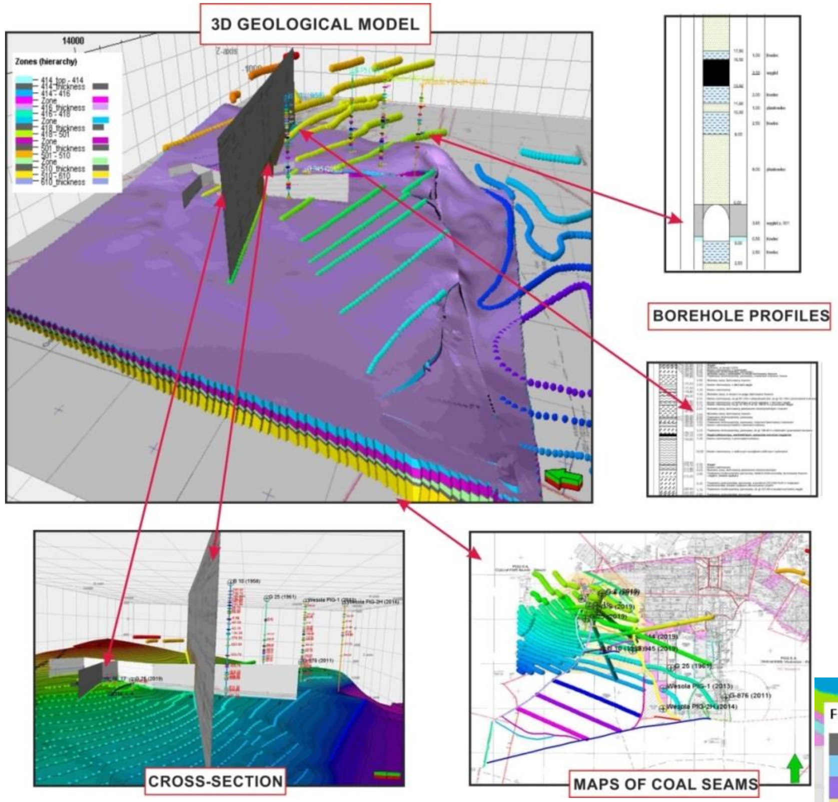

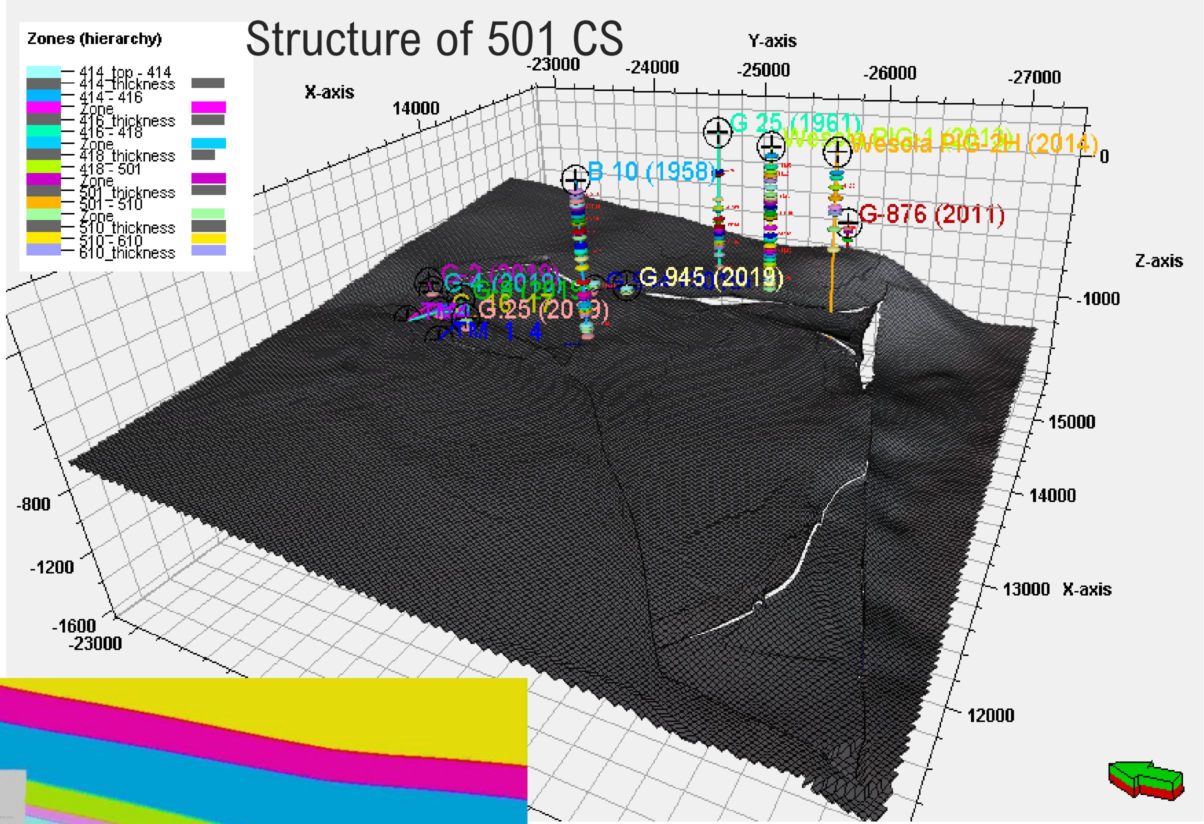

Horizontal resolution 25 x 25 m

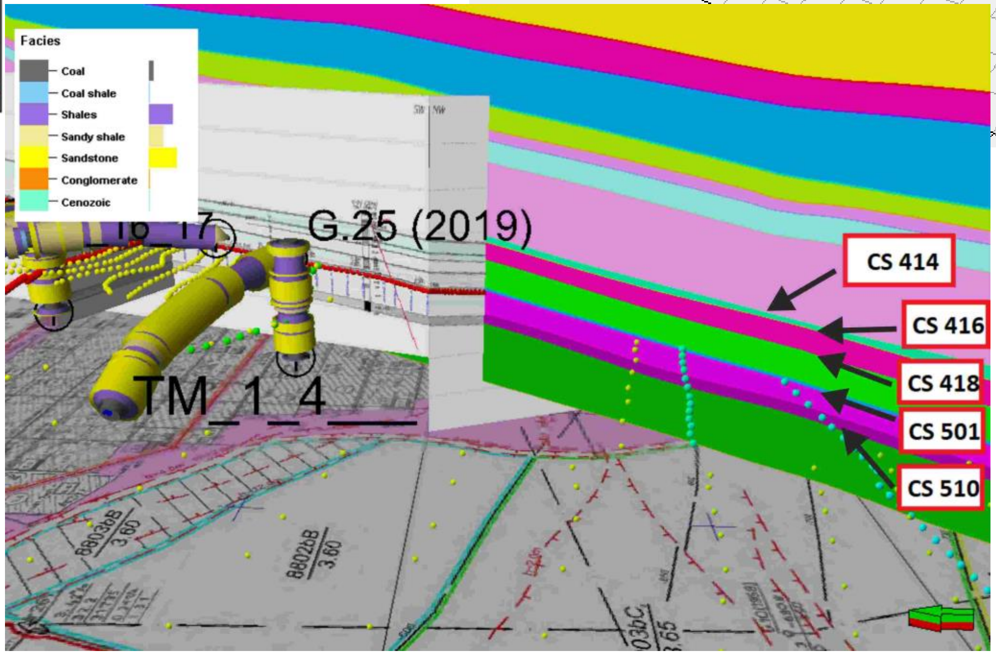

- Development of large scale and high resolution 3D structural models depicting tectonic settings, geometry of main structural surfaces and thickness of particular lithological units

Structural model of the strata between 610 and 414 coal seams

3D PARAMETRIC MODEL

Development of large scale lithotype model driving parametric models of petrophysical and geomechanical properties.

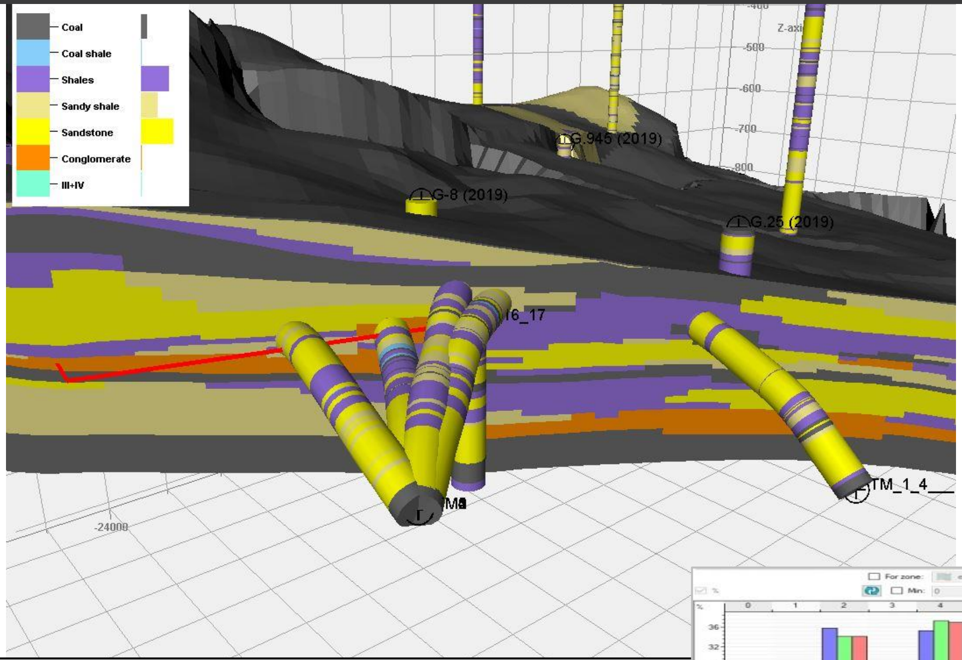

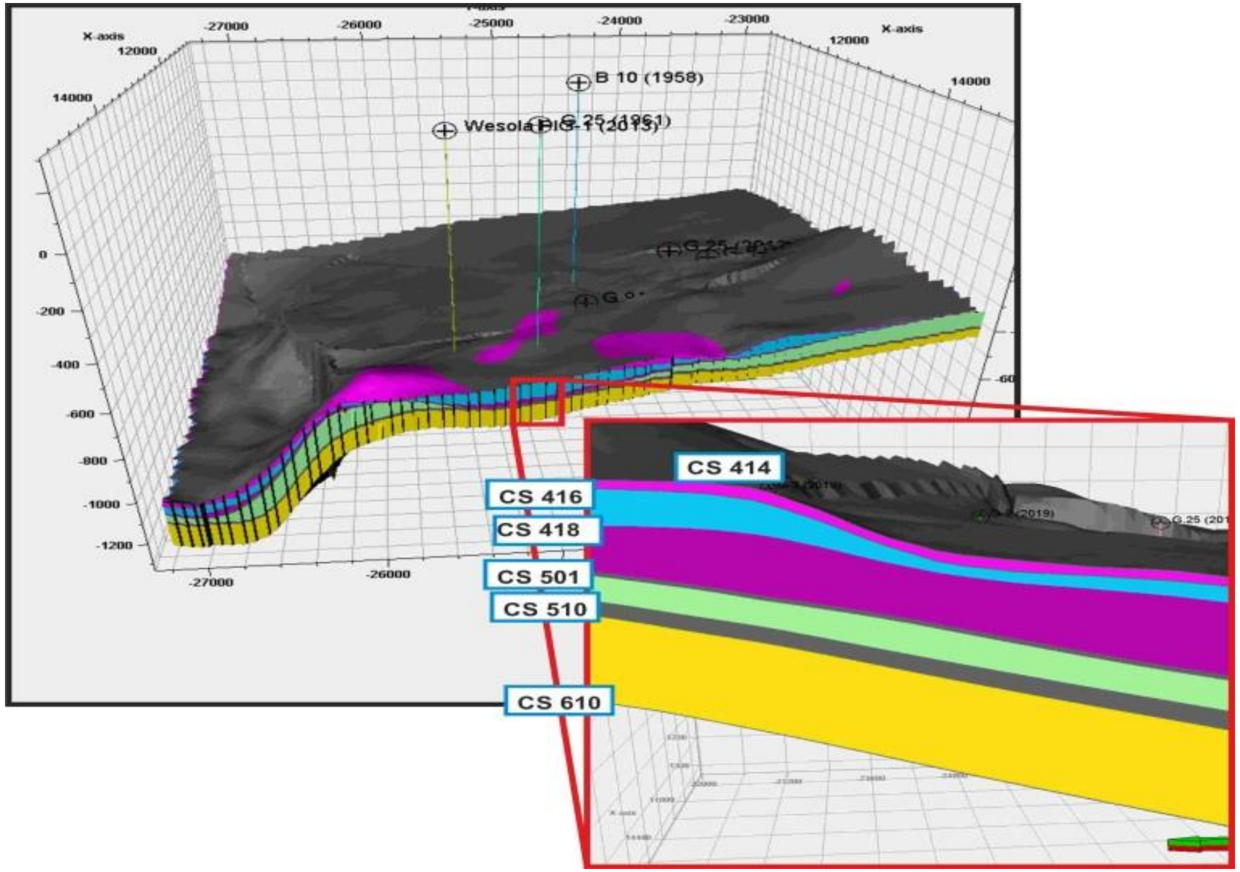

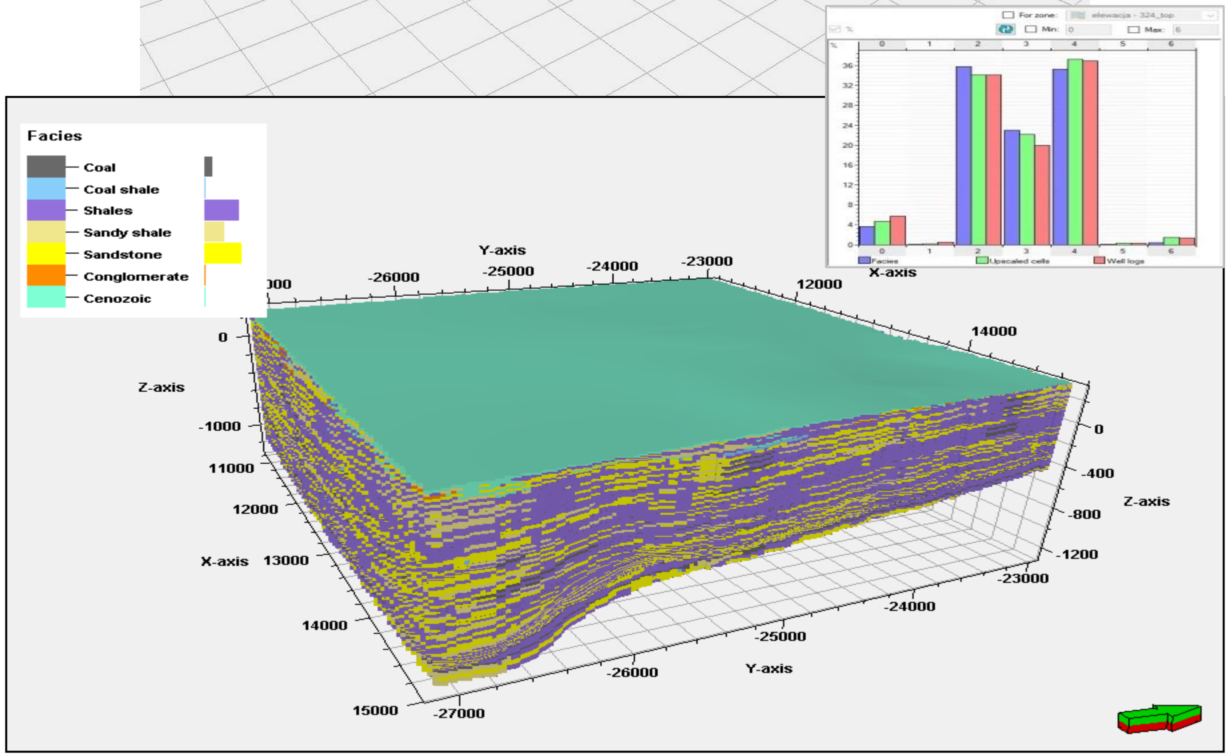

3D PARAMETRIC MODEL – PETROPHYSICAL PROPERTIES

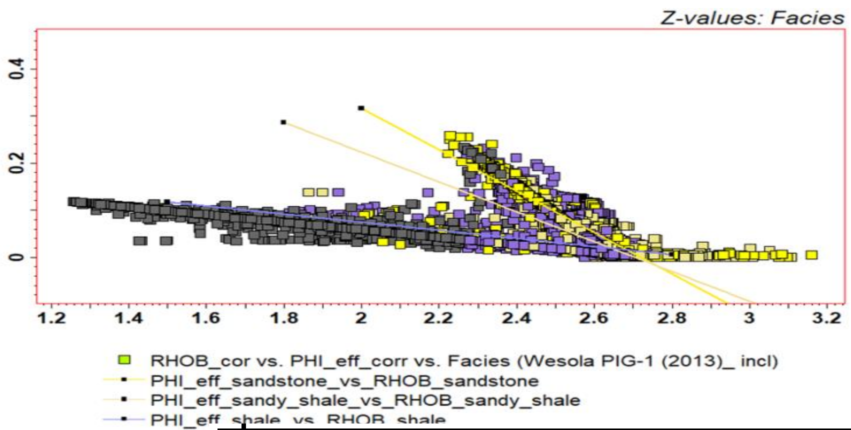

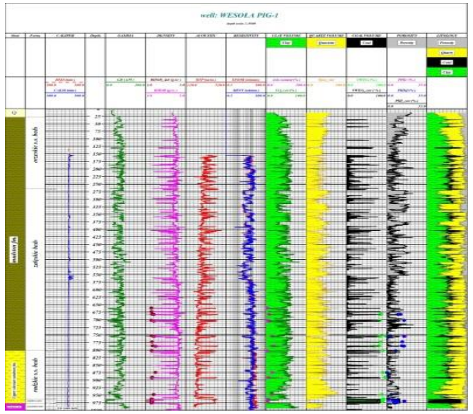

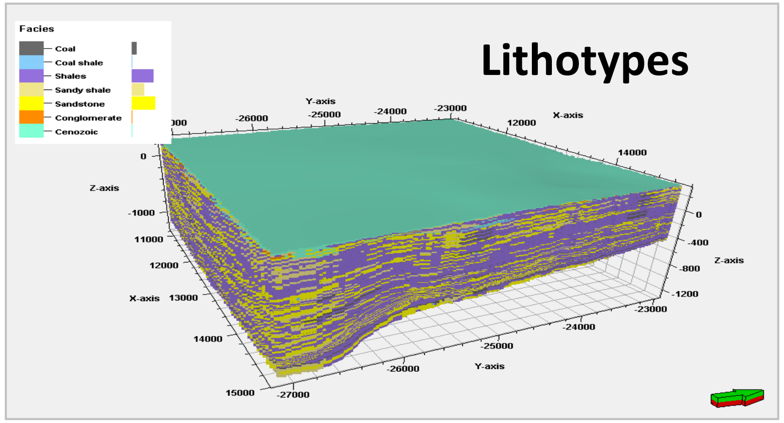

Lithotype	Shale	Sandy shale	Sandstone
Linear function	PHI_eff = -0.0860927 * RHOB + 0.246791	PHI_eff = -0.316526 * RHOB + 0.855864	PHI_eff = -0.438728 * RHOB + 1.19334
Correlation coefficient	-0.55	-0.76	-0.87

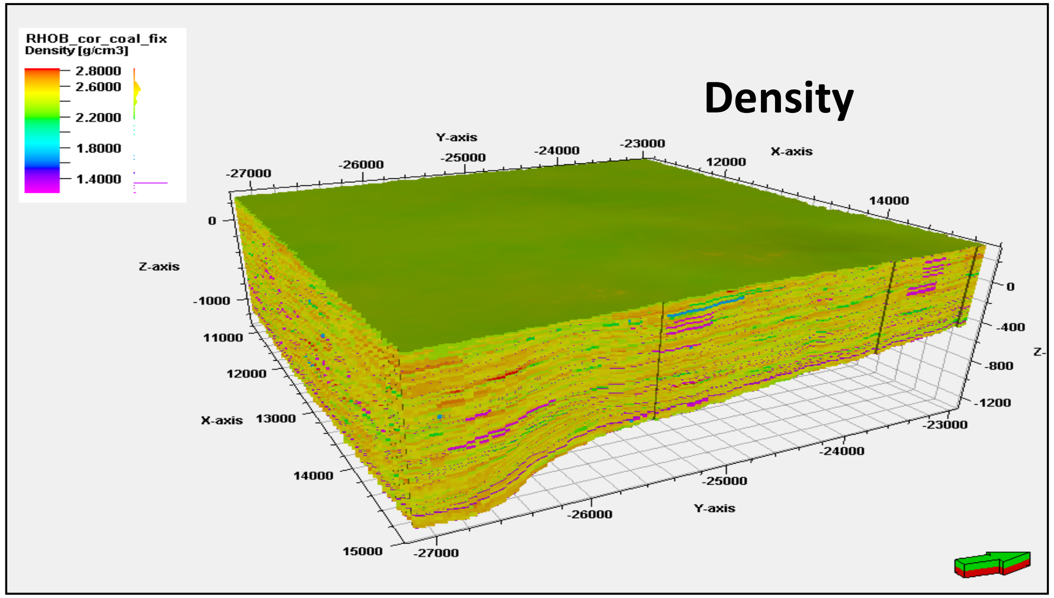

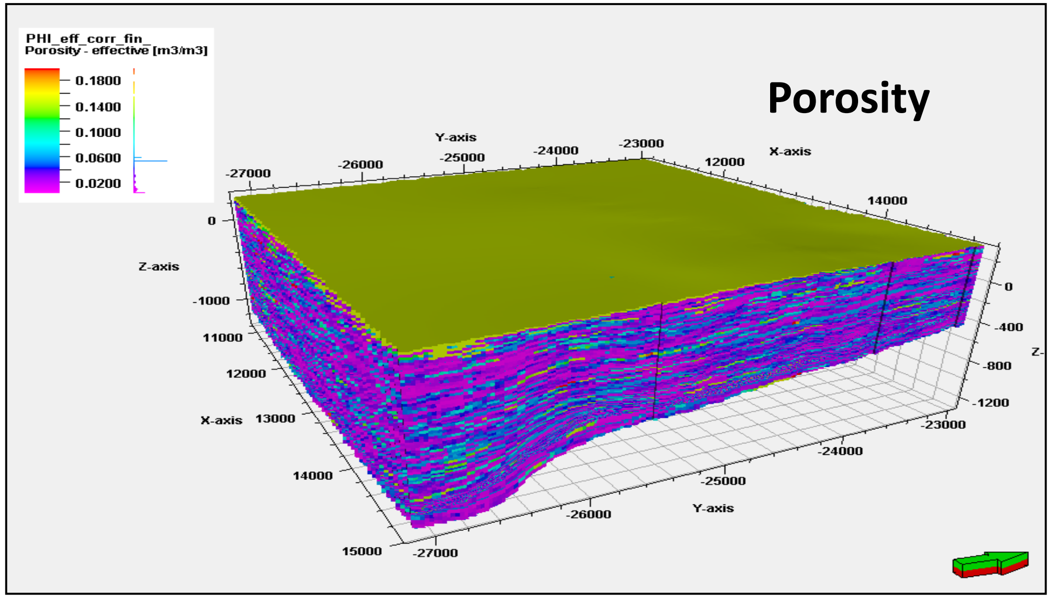

Fig. 4.Petrophysical large scale models of the C field strata between top surface and 610 CS in the Murcki-Staszic coal mine

3D PARAMETRIC MODEL – GEOMECHANICAL PROPERTIES

Lithotype/ parameter	Young modulus	Poisson ratio	UCS
Sandstone	$E_{stat}=1.1211*E_{dyn}-23.15$ (Xu et al, 2016)	$PR_{stat}=1.135*PR_{dyn}-0.063$ (Xu et al, 2016)	$UCS=3.3991*E_{stat}+63.69$ (Xu et al, 2016)
Sandy shale	$E_{stat}=1.170*E_{dyn}-24.36$ (Xu et al, 2016)	$PR_{stat}=1.435*PR_{dyn}-0.078$ (Xu et al, 2016)	$UCS=1.476*E_{stat}+70.479$ (Xu et al, 2016)
Shale	$E_{stat}=0.076*v_p$^3.23 (Horsud, 2001)	$PR_{stat}=1.108*PR_{dyn}-0.058$ (Slota-Valim, 2015)	$UCS=1.001\varphi$^−1.143 (Chang, et al, 2006)

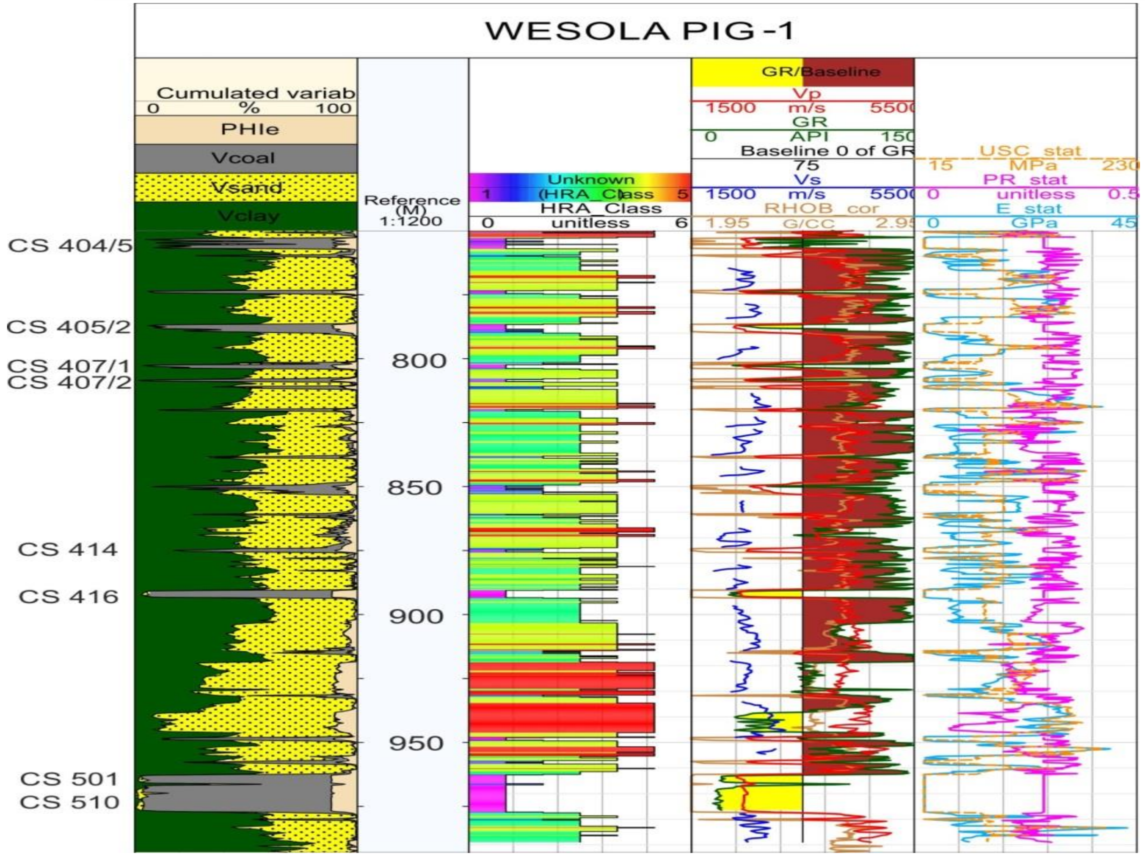

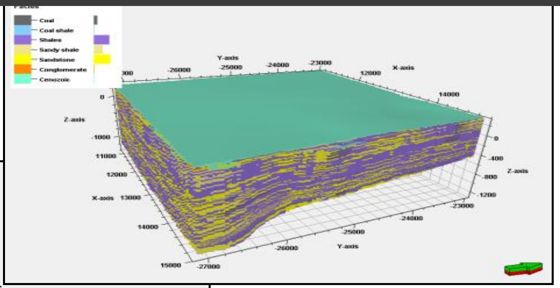

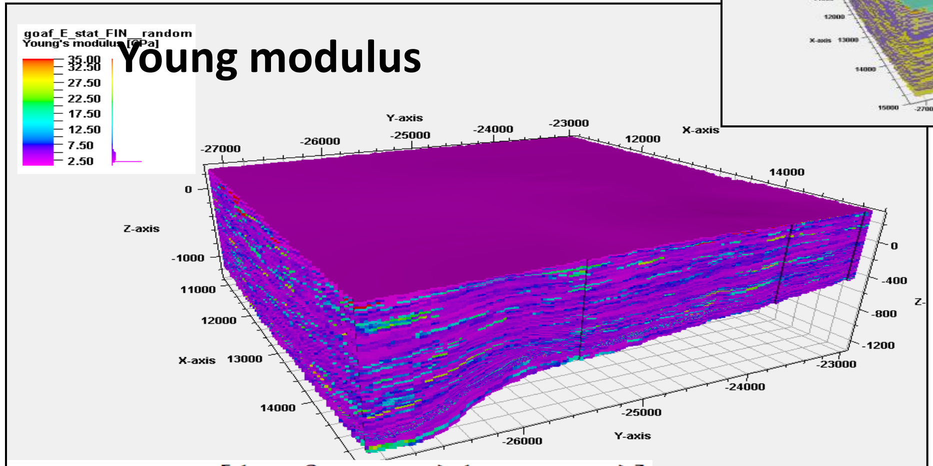

$$E_{dyn} = \rho\, v_s^2[(3v_p^2 - 4v_s^2)(v_p^2 - v_s^2)]$$

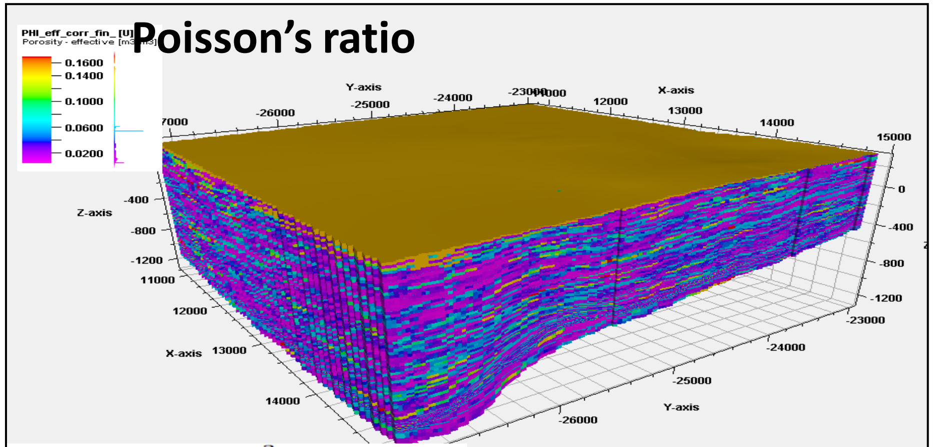

$$v_{dyn} = v_p^2 - \frac{v_s^2}{2}(v_p^2 - v_s^2)$$

Figure. Diagram presenting the lithological model (track 1), HRA based lithotypes (coal – marked in pink, sandstones in red, shales in green sandy shales in green-yellow (track 3), input data (GR - Gamma Ray, vp - compressional velocity, vs - shear wave velocity, ρ - density) (track 4) and calculated static mechanical parameters (UCS –marked with orange dashed line, Young modulus – marked with blue line and Poisson ratio – marked with pink continuous line).

3D PARAMETRIC MODEL – GEOMECHANICAL PROPERTIES

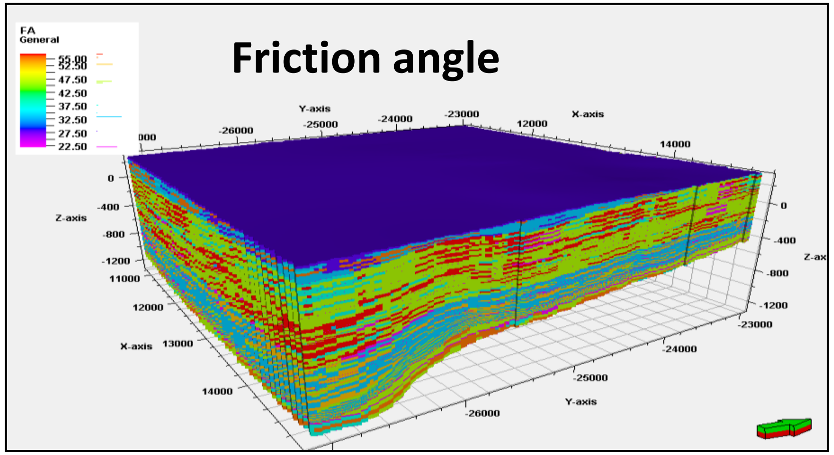

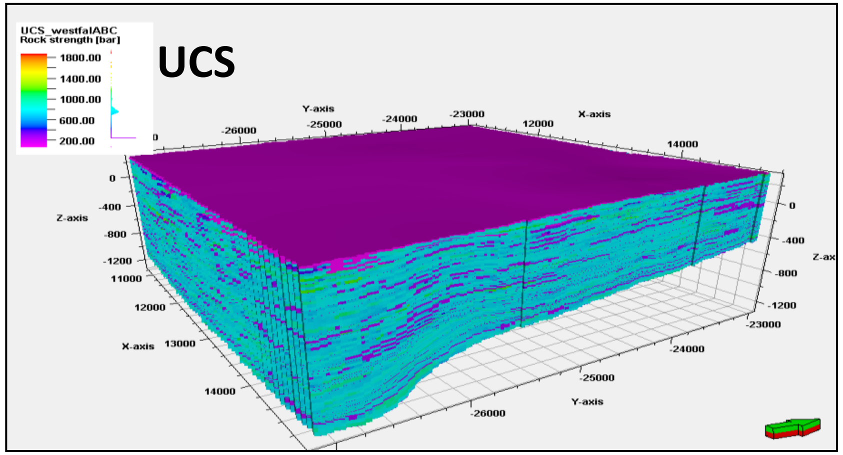

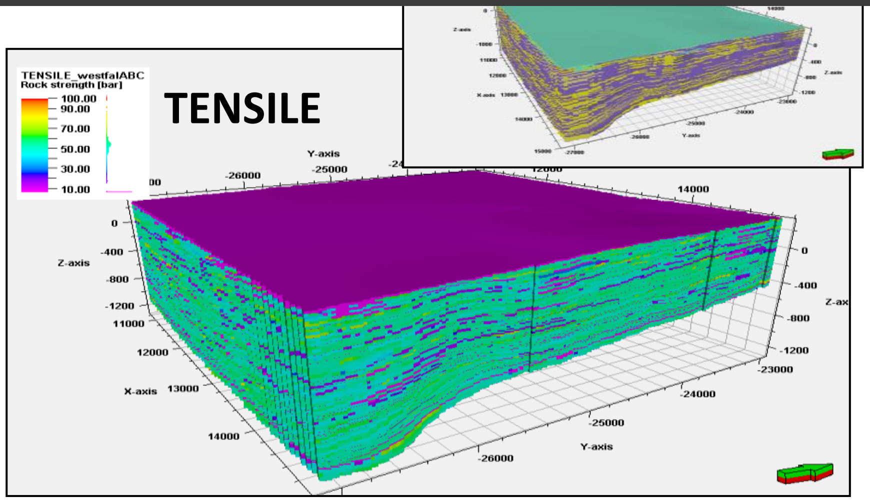

Parametr	Q+III	Conglomerate (Jacobsen, 1943)	Coal	Goaf	Coal shale Malkowski, 2008	Shale: Westfal A CS 300	Shale: Namur C CS 400	Shale: Namur B PCS 500	Sandy shale: Westfal A CS 300	Sandy shale: Namur C CS 400	Sandy shale: Namur B CS 500	Sandstone: Westfal A CS 300	Sandstone: Namur C CS 400	Sandstone: Namur B CS 500
E [GPa]	**0.8** Zhu et al., 2019	**41**	**2.08** WP2	**1.77**	**5** Malkowski, 2008	**1.424-6.79 av 4.69** (KWK-M-S archival data)			**3.94-6.89 av. 5.14** (KWK-M-S archival data)			**4.09-8.18 av 5.73** (KWK-M-S archival data)		
PR	**0.35** Zhu et al., 2019	**0.25**	**0.29** WP2	**0.27**	**0.28** Malkowski, 2008	**0.07-0.37 av 0.16** (KWK-M-S archival data)			**0.06-0.3 av 0.14** (KWK-M-S archival data)			**0.07-0.2 av 0.12** (KWK-M-S archival data)		
UCS [MPa]	**6.9** Zhu et al., 2019	**40**	**24.6** WP2	**12.3**	**28.78** Malkowski, 2008	**22.6-51.4**	**31.7-61.8**		**8-31.7**	**24.8-47.6**		**14-36.1**	**39-56.3** (KWK-M-S archival data)	
TENSILE	**0.69**	**4**	**0.6** WP2	**1.23**	**2.88**	**0.29-4.42 av 1.47** (KWK-M-S archival data)			**1.23-3.82 av 2.15** (KWK-M-S archival data)			**1.15-4.55 av 2.82** (KWK-M-S archival data)		
DENS	Well log	Well log	WP2	**1.14**	**2.14**	Well log	Well log	Well log	Well log	Well log	Well log	Well log	Well log	Well log
PORO	Well log	Well log	WP2	**30**	Well log	Well log	Well log	Well log	Well log	Well log	Well log	Well log	Well log	Well log
FA	**28** (Ortuz, 1986)	**35** (Jacobsen, 1943)	**22** (Szott et al., 2018)	**30**	**33.5** (Godula, 1984)	**46.5** (Godula, 1984)	**33.5** (Godula, 1984)	**46.5** (Godula, 1984)	**37.5** (Godula, 1984)	**46** (Godula, 1984)	**37.5** (Godula, 1984)	**57** (Godula, 1984)	**53** (Godula, 1984)	**55.5** (Godula, 1984)
BIOT	**1**	**1**	**1**	**1**	**1**	**1**	**1**	**1**	**1**	**1**	**1**	**1**	**1**	**1**

Based on well log data; KWK M-S archival data; WP2 data; Zhu et al., 2019; Ortuz, 1986; Jacobsen, 1942; Szott et al., 2018; Malkowski, 2008; Godula, 1984)

INITIAL STRESS AND STRAIN IN REGIONAL MODEL

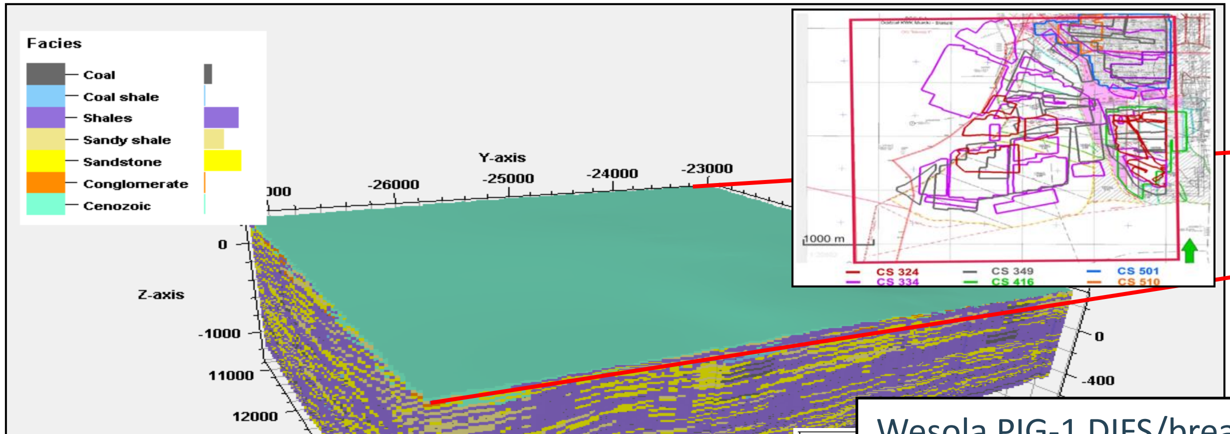

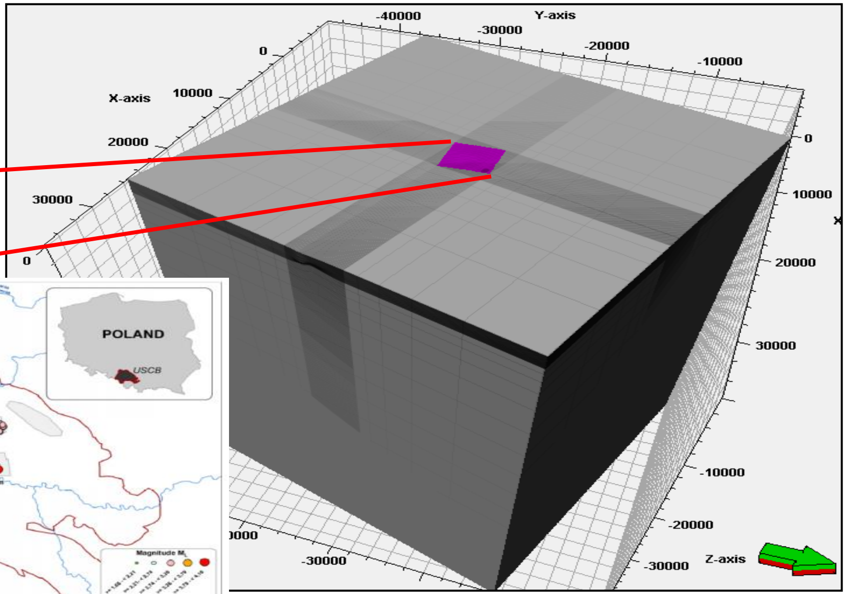

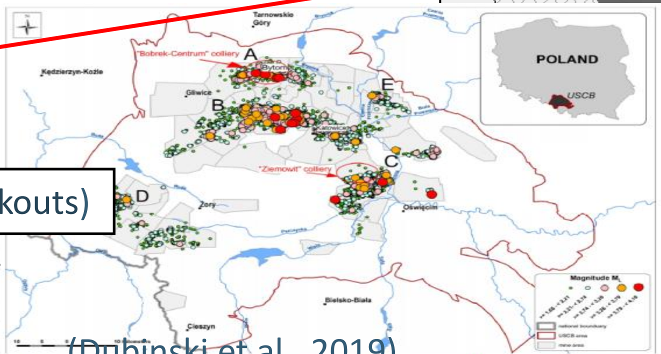

(Dubinski et al., 2019)

Fig. 2. Map of the USCB showing the epicenter locations of strong tremors ($M_L \geq 1.7$) for the 1977-2016 period (A: Bytom trough, B: main anticline, C: main trough, D: Jejkowice trough and Jastrzębie folds, E: Kazimierz trough)

Wesola PIG-1 DIFS/breakouts)

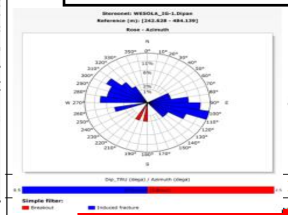

Parameters	Value
...mum stress axis, σ_1	297°/79°
intermediate stress axis, σ_2	99°/11°
minimum stress axis, σ_3	189°/3°
stress ratio, R	0.17
[illegible]	[illegible]
mean fault angle ± std. deviation	12.3° ± 9.2°
mean friction angle, Φ	29°
mean shear stress, τ ± std. deviation	0.31 ± 0.01
shortening/extension (trend/plunge)	355°/82°

Fig. 4. Geomechanical large – scale model of the C field in the Murcki-Staszic coal mine

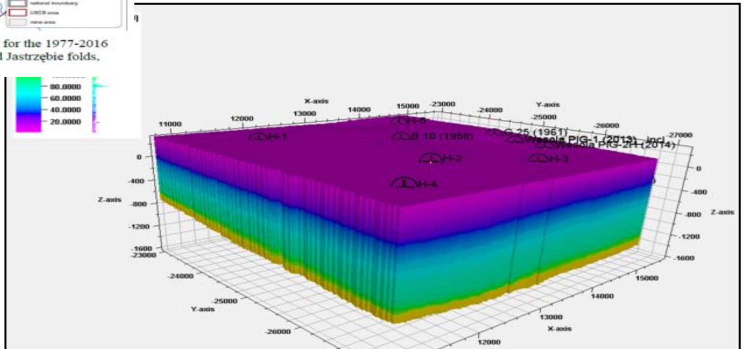

Pore pressure

- ✓ 3D geomechanical model of the C field in Murcki – Staszic coal mine
- ✓ Determination of boundary conditions:
- ✓ Stress regime: normal faulting, $\sigma_v > \sigma_H > \sigma_h$ *(Zuberek et al., 1997)*, ***σ3/ σ1=0.17***, ***σH*** *azimuth =* ***99*** *deg (Dubinski et al., 2019)*
- ✓ Calculation of stress and strain field in initial geological conditions prior to the mining activity in the large scale model
- ✓ Calculation of stress and strain field in mining conditions affected by the mining activity (large scale model)

Tab 2. Content of solids dissolved in underground water in Carboniferous productive intervals changing with depth (based on Różkowski et al., 1990).

(Rozkowski et al., 1990)

Detph	Average value (mg/dm3)	Pressure gradient
0-200	3349,45	0,100018008
200-400	13941,45	0,101077029
400-600	51836,07	0,104865849
600-800	76887,38	0,107370556
800-1000	117377,12	0,111418844

3D PARAMETRIC MODEL – LOCAL-SCALE MODELS

3D structural model

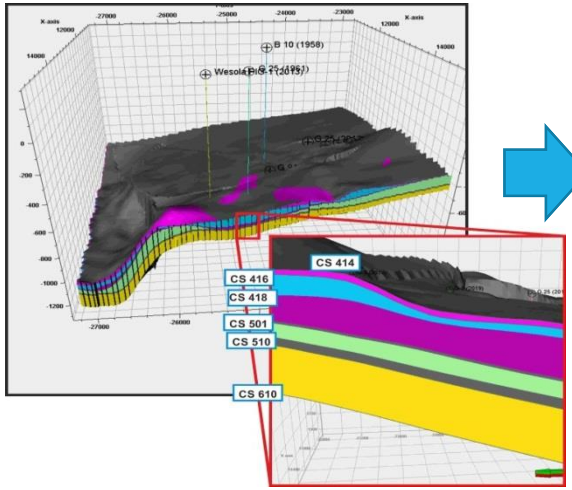

Facies model

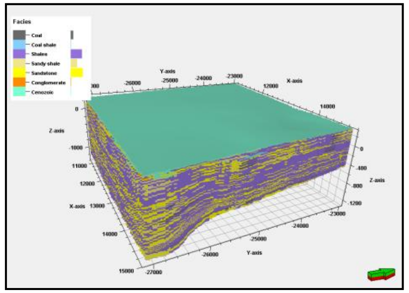

Statistical relationships

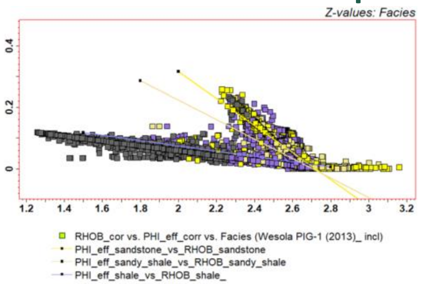

1 D models

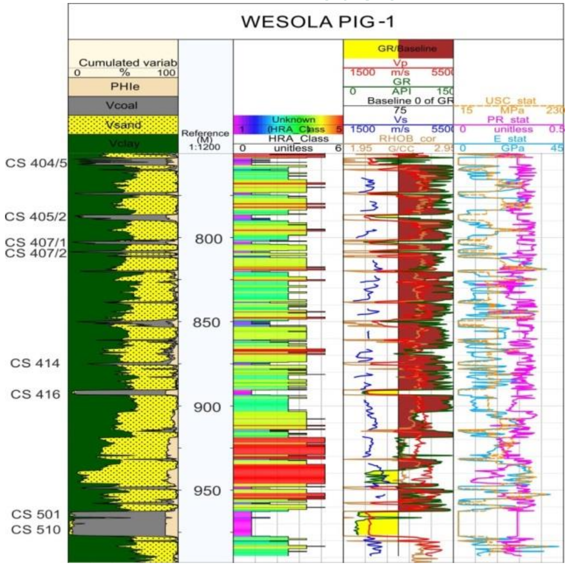

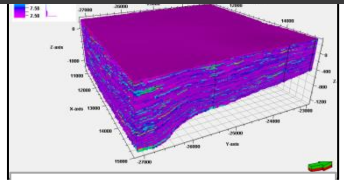

Elastic properties (E, ν)

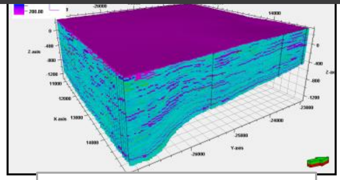

Strenght properties (UCS, FA, TENS)

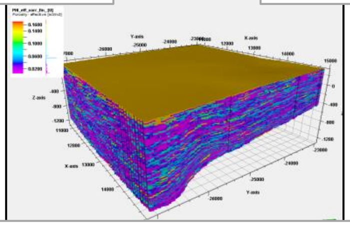

Petrophysical properties (ρ, ϕ, k)

3D local parametric models

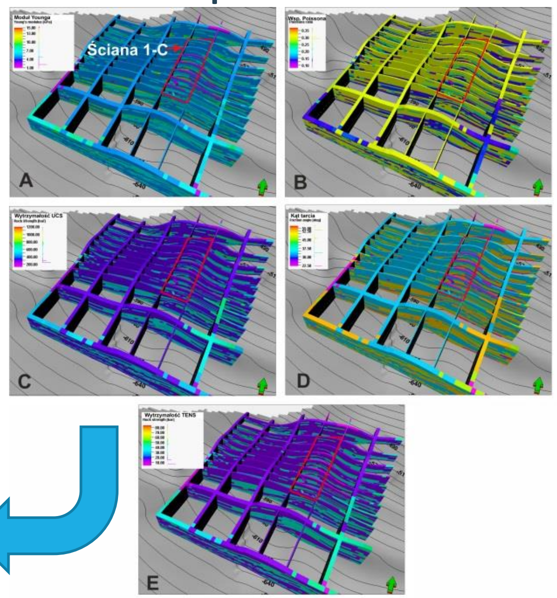

Geomechanical simulations

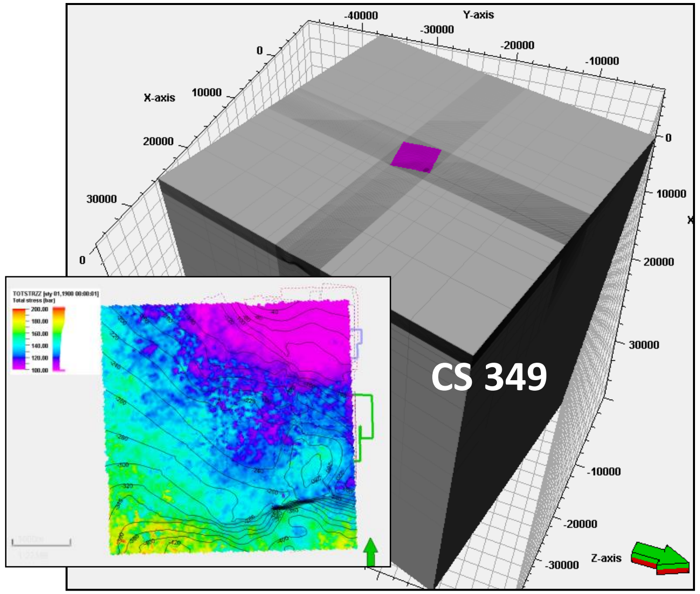

ε, σ field

- 3D geomechanical and parametric models of the C field in Murcki – Staszic coal mine (large scale) and local models of drainage area
- Determination of boundary conditions:
- Stress regime: normal faulting, $\sigma_v > \sigma_H > \sigma_h$ *(Zuberek et al., 1997),* ***σH/σh= 1.25*** *(Jarosinski, 2005),* ***σH*** *azimuth =* ***99*** *deg (Dubinski et al., 2019; analysis of damage zones in Wesola PIG-1 borehole)*
- Calculation of stress and strain field in initial geological conditions prior and due to the mining activity in the large scale model
- Calculation of stress and strain field in mining conditions affected by the mining activity (large scale model)

DD-MET

EFFECTIVE COUPLING OF FLOW AND GEOMECHANICAL SIMULATIONS

PROBLEM: Simultaneous flow and geomechanical simulations – **complex** simulation modelling of very high computational costs

CONVENTIONAL APPROACH: **External coupling** between separate simulations of fluid flow evolution (pressure and saturation distributions) and static geomechanical state (strain and stress tensor distributions) by best available flow and geomechanical simulators, respectively – **iterative method** supplemented with **correlations** between rocks transport properties and their geomechanical state – until appropriate consistency achieved

Effectiveness of the approach, depending on the rates of geomechanical and transport properties variations, may result in **work– and time– consuming runs**

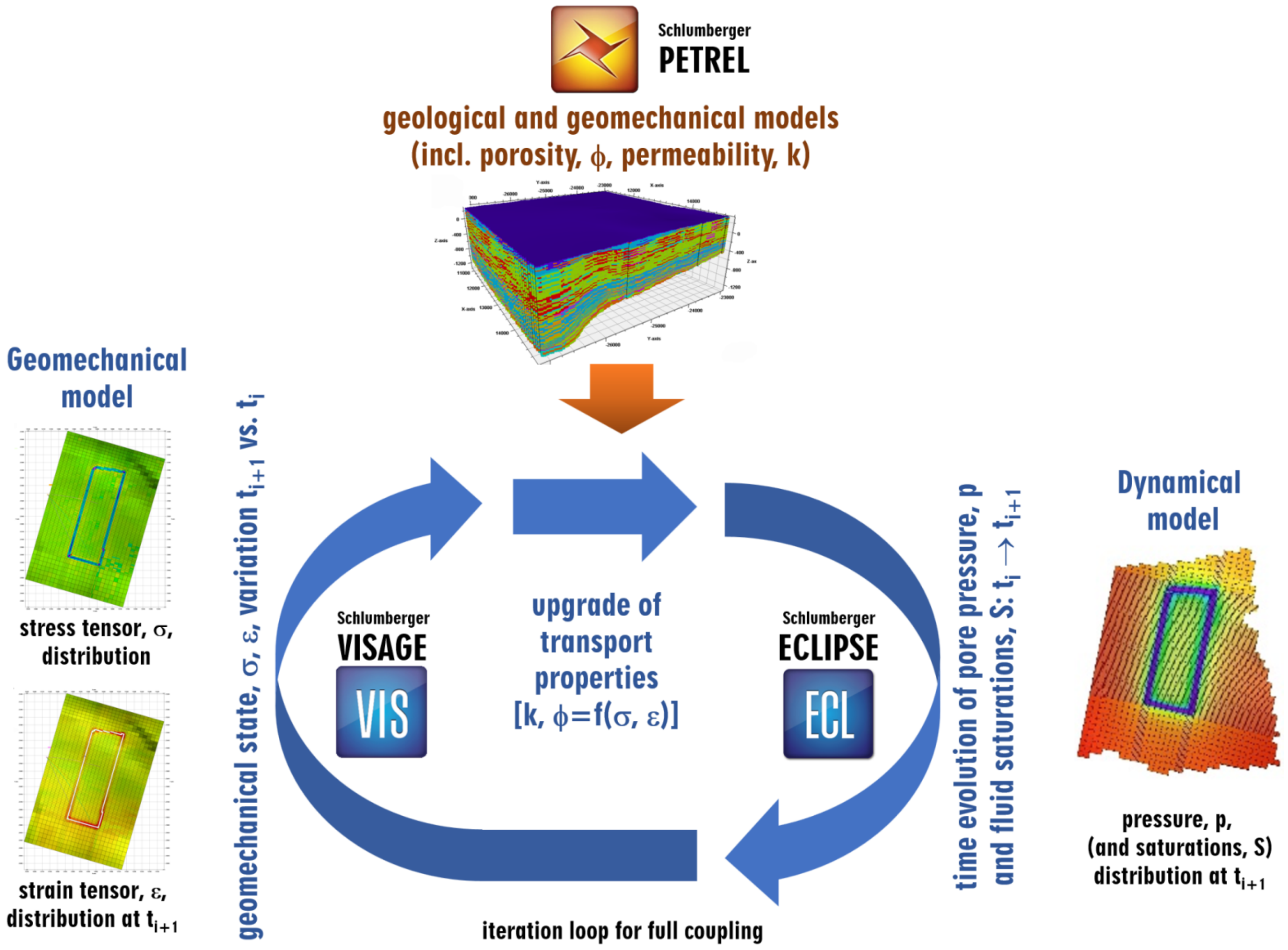

Flow diagram of conventional simulation coupling

EFFECTIVE COUPLING OF FLOW AND GEOMECHANICAL SIMULATIONS

ALTERNATIVE SOLUTION: Effective coupling by **local correlations** between reservoir **pressure variations (ΔP)** and modifications of rock transport properties from **geomechanical effects (Δε, Δσ)** and their **correlations with transport properties (ΔT, ΔPV)** at **specific time intervals** including continous flow and geomechanical variations: **ΔP → Δε, Δσ → ΔPV, ΔT** – **maximum implicite approach**

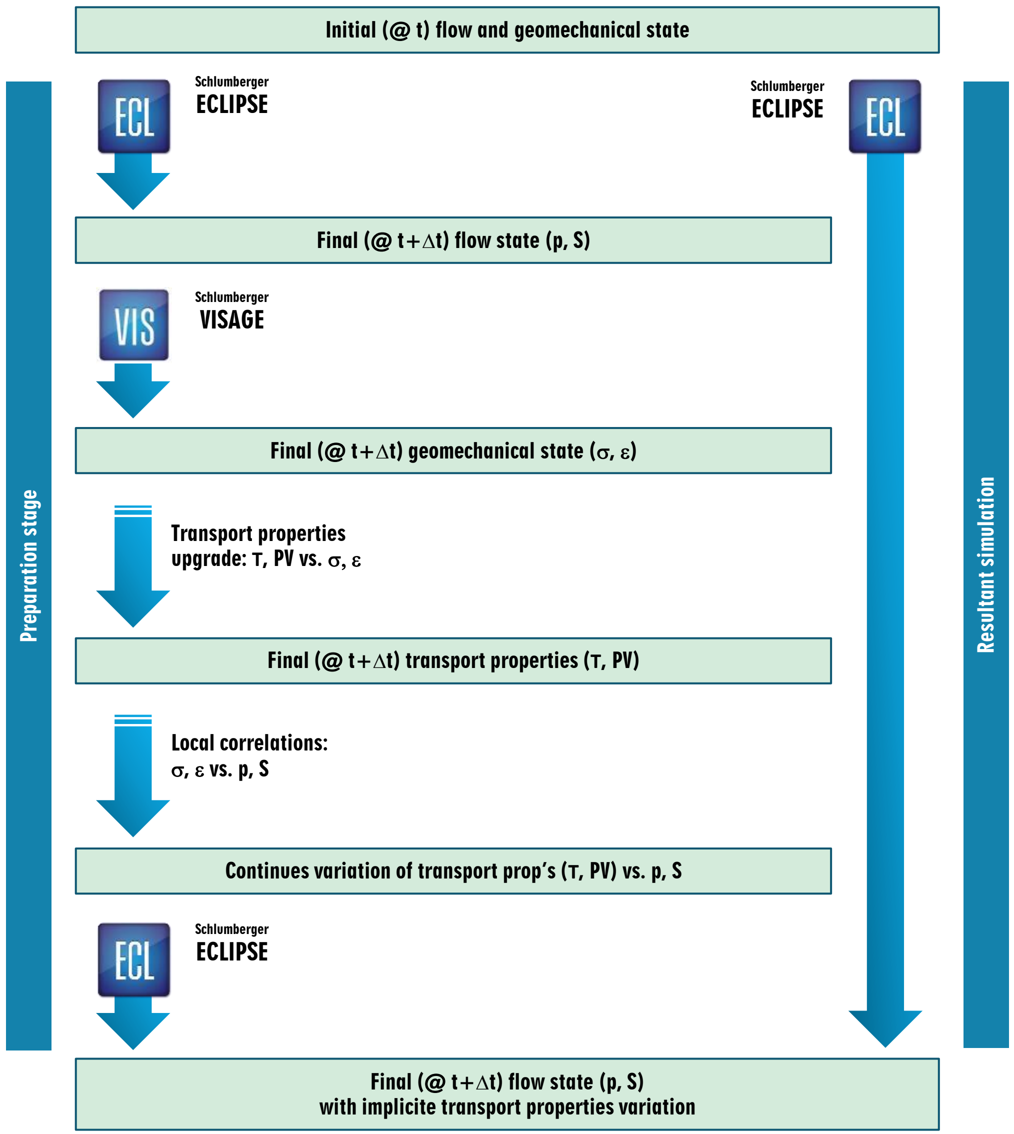

Flow diagram of simulation effective coupling

GEOMECHANICAL EFFECTS UPON ROCK PROPERTIES

Geomechanical state variations during coal mining:

- elastic deformations due to pressure reduction – continuous variations – global (model) range – implicit simulations
- plastic deformations due to excavation activities – (model) discrete variations – local range – explicit simulations
- rock (coal) failure – (model) discrete variations – local range – explicit simulations

Effects of geomechanical state variations upon transport properties of rocks:

- porosity, ϕ (pore volume, PV) modifications due to elastic and plastic deformations
- permeability, k (transmissibility, T) modifications due to elastic and plastic deformations
- diffusion rate increase due to rock (coal) failure

EFFECTS OF CONTINOUS DEFORMATIONS

Effective correlations between reservoir pressure variations (ΔP) and rock transport properties (ΔT, ΔPV) implicitely applied in simulation process and combined from:

- local correlations between reservoir pressure variations (ΔP) and modifications of rock transport properties from geomechanical effects (Δε, Δσ)
- correlations between geomechanical state variations (Δε, Δσ) and rock transport properties (ΔT, ΔPV), e.g. Kozeny-Carman isotropic model

$$\Delta\phi = \alpha\Delta\epsilon_v$$

$$T_i = T_{0i}\frac{\phi^3/(1-\phi)^2}{\phi_0^3/(1-\phi_0)^2}$$

where:

T_i = modified transmissibility in i−th main direction,
T_{0i} = initial transmissibility in i−th main direction
ϕ = modified porosity,
ϕ_0 = initial porosity,
$\Delta\phi$ = change in porosity,
$\Delta\epsilon_v$ = change in volumetric strain,
α = Biot's coefficient

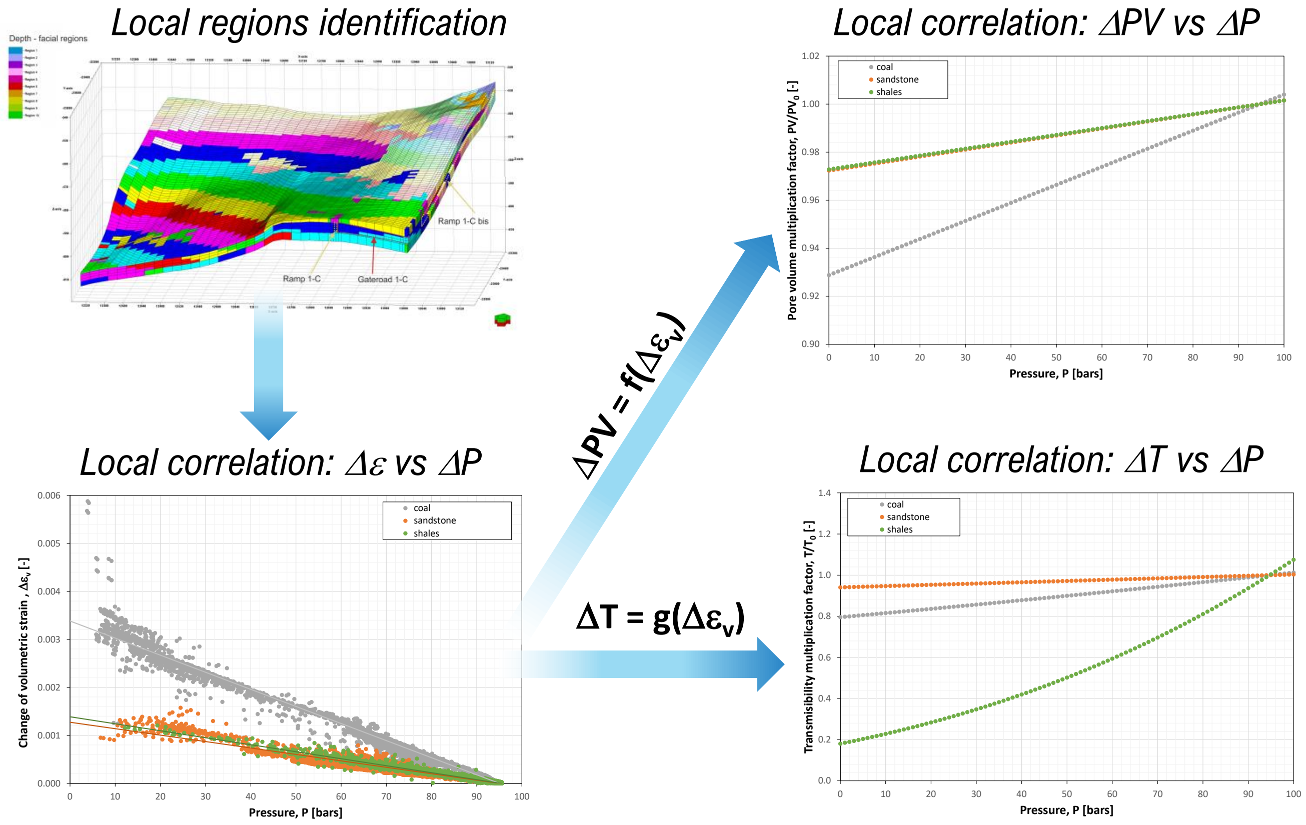

EFFECTS OF DISCRETE DEFORMATIONS

Step-like modifications of rock transport properties (ΔT, ΔPV) explicitly introduced into simulation process and determined from correlations between the properties and geomechanical state modifications ($\Delta\varepsilon$, $\Delta\sigma$), e.g.

Durucan and Shi anisotropic model

$$T_i = T_{0i}\, e^{-c \sum_{j=1}^{3} \Delta\sigma_j (1-\delta_{ij})}$$

where:

T_i = modified permeability in i–th main direction,
T_{0i} = initial permeability in i–th main direction,
c = permeability compressibility,
$\Delta\sigma_j$ = change in effective stress in j–th main direction,
δ_{ij} = Kronecker delta

DISCRETIZATION OF THE SIMULATION PROCESS

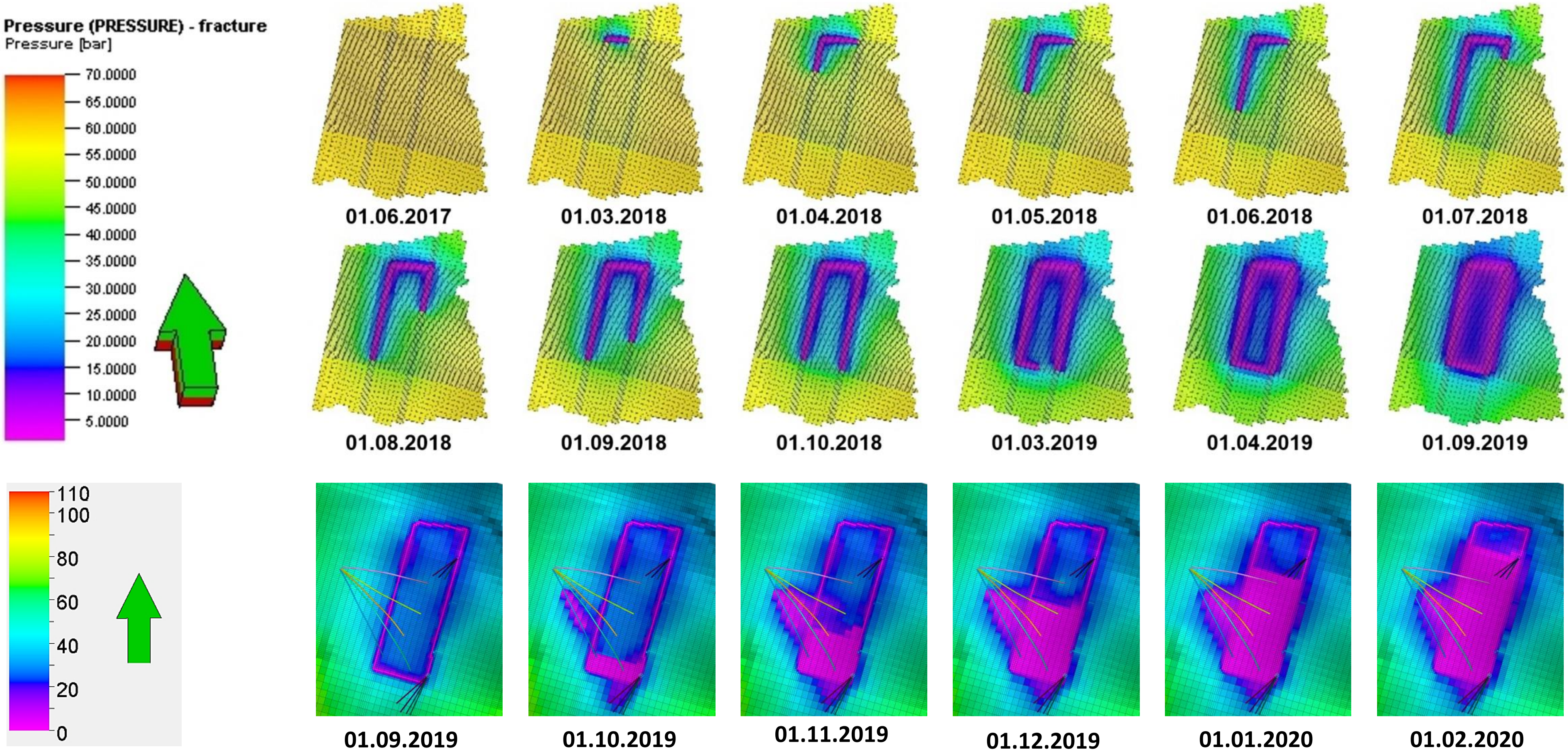

DISTRIBUTION OF STRESS TENSOR VARIATIONS ($\Delta\sigma_{ii}$, ii = xx, yy, zz) ALONG VERTICAL CROSS SECTIONS AT HALF TIME

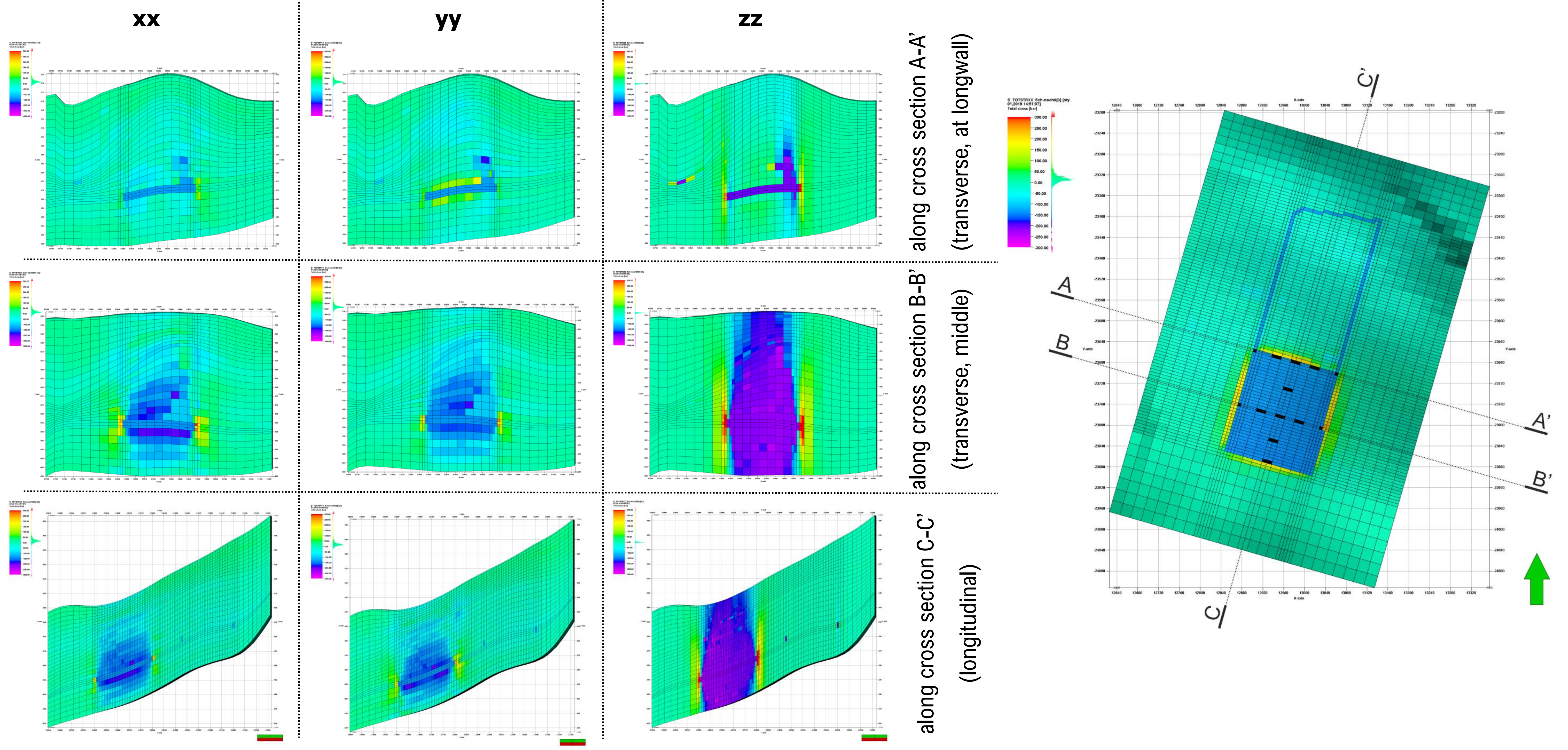

HISTORY MATCHING

○○ observed data - directional wells
simulation result - directional wells

Ventilation data

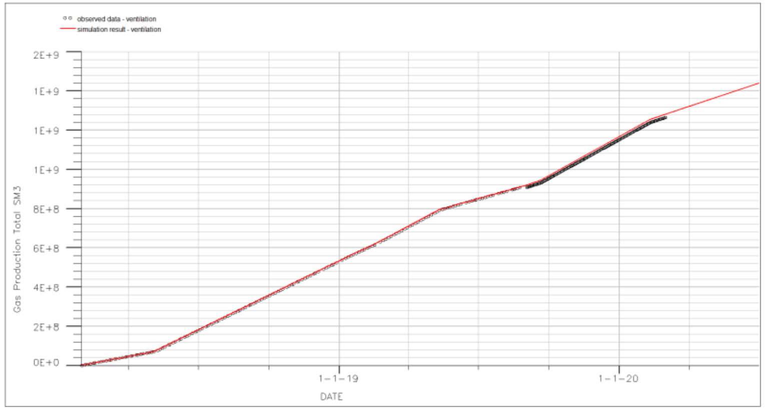

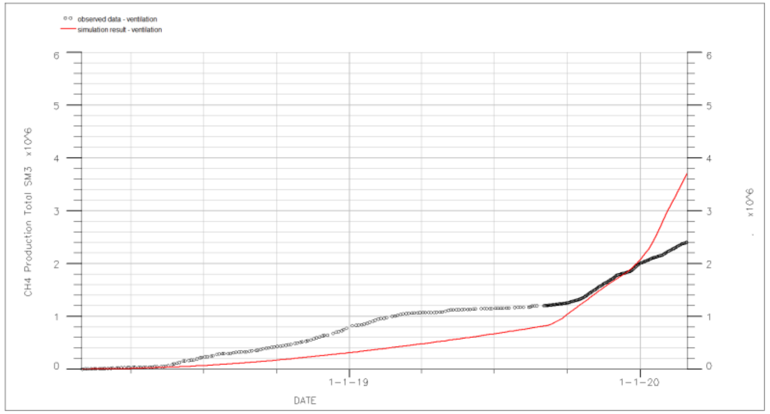

Directional wells

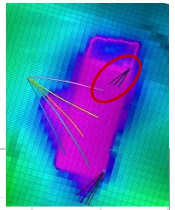

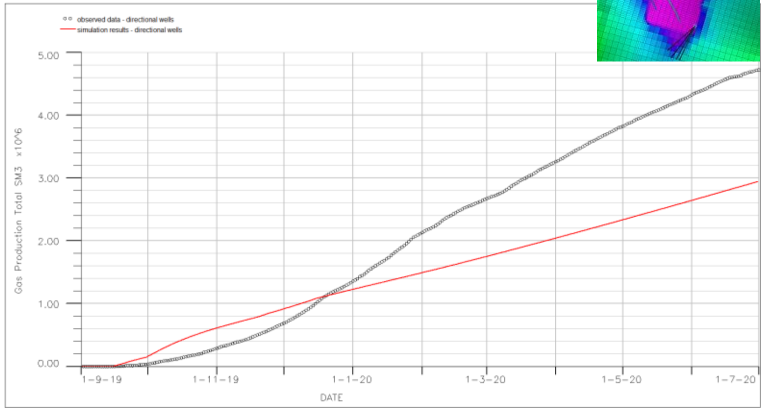

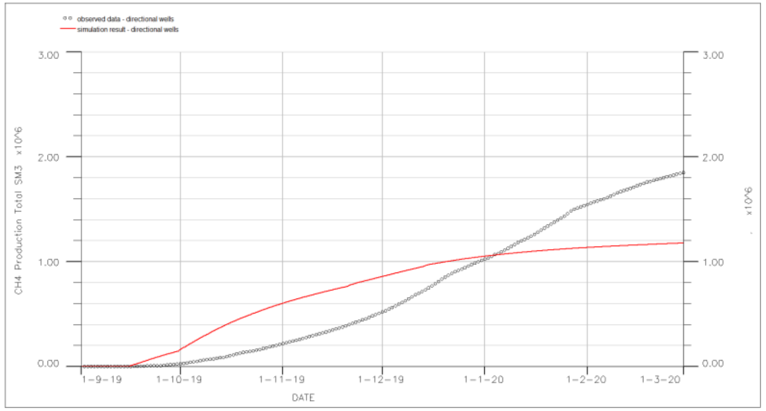

Conventional wells

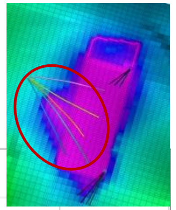

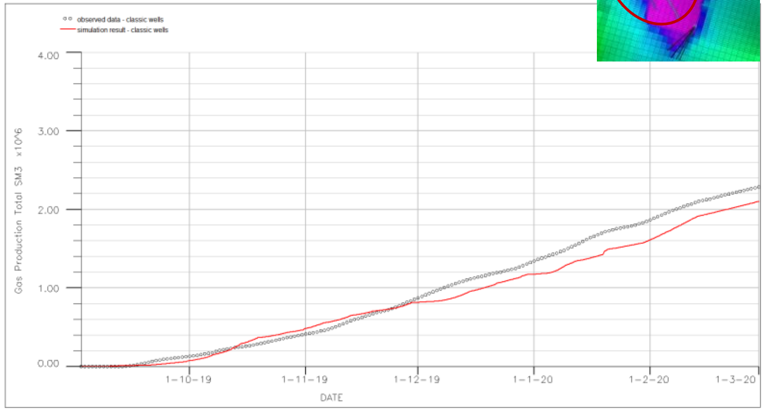

gas

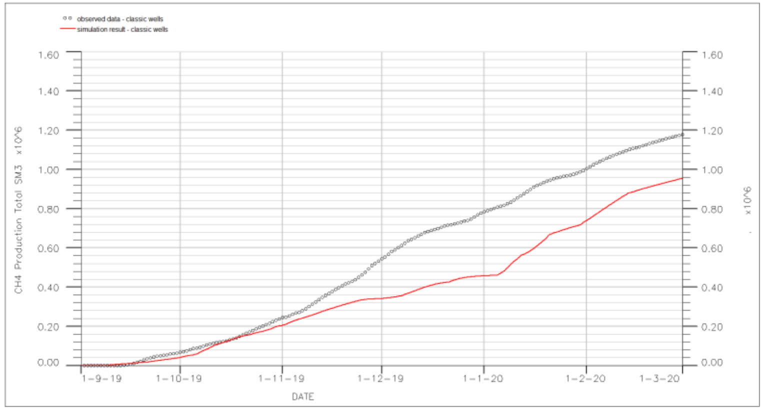

methane

SUMMARY AND CONCLUSIONS

- To assess the effectivness of the aplied drainege technology a numerical methods coupling geomechanical and fluid flow models were used

- The method proposed in the studies and comprising effectively coupled geomechanical and dynamical simulations of reservoir region and its extension allows to take into account impact of geomechanical effects ($\Delta\varepsilon$, $\Delta\sigma$) upon transport properties of reservoir rock (ΔPV, ΔT) at various considered stages including gate road excavations, long wall movement or drilling conventional and LRDD including continuous flow and geomechanical variations: $\Delta P \rightarrow \Delta\varepsilon, \Delta\sigma \rightarrow \Delta PV, \Delta T$

- the quantitative results of those geomechanical effects depend upon detailed properties of both geomechanical state evolution and geological characteristics of the coal seam and surrounding strata,
- the following 2 correlations are key factors when the effective transport properties of the rock are concern:

  the correlation between geomechanical state (stress and strain field) and

  and rock transport properties Kozeny – Carman (isotropic model) and Durucan and Shi (anisotropic model)

- The dynamic models are in the stage of calibration to achieve comparable drainage effectiveness as it was reported by the coal mine operator. The matching is not easy due to several factors: the quality of the data obtained from the mine, geomechanical effects hindering the flow of methane to the directional wells - stress shadow effect, and the complicated trajectory of the boreholes, as well as complex lithotypes spatial distribution. Finally, it is worth mentioning that the calibration process is not finished as the project is still ongoing.

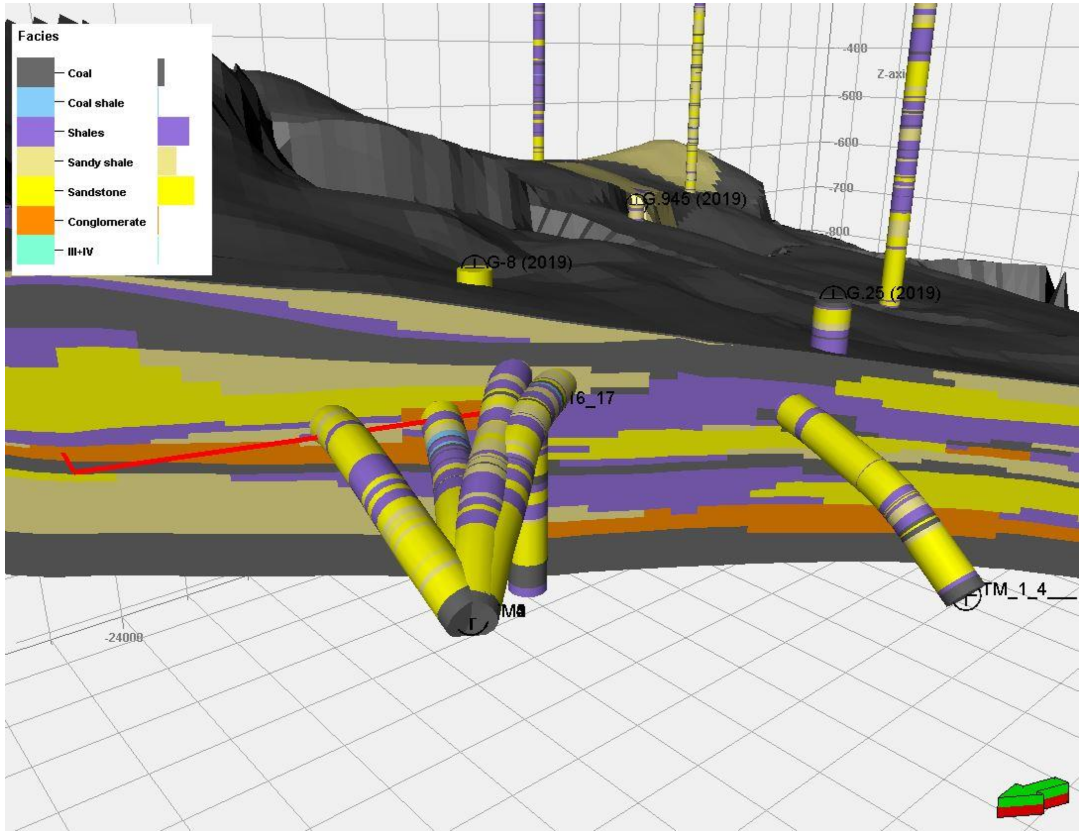

THANK YOU FOR YOUR ATTENTION

DD-MET

The presented work received funding from the European Commission Research Programme of the Research Fund for Coal and Steel Technical Group Coal 1 TGK1 Grant Agreement number: 847338 — DD-MET RFCS-2018/RFCS-2018